

# DYNAMICS OF ROTORS WITH CRACK IN SHAFTS

©2014 Degtiarev S.A.<sup>1</sup> Kutakov M.N.<sup>1</sup>, Leontiev M.K.<sup>2</sup>

<sup>1</sup>Engineering and consulting center for dynamic problems Alfa-Tranzit., Co.Ltd, Khimky, Russia

<sup>3</sup>Bauman Moscow State technical university, Moscow, Russia

## Annotation

The authors give the methodology and the algorithm where crack is simulated by variable coefficient of moment flexibility obtained for the local section of the shaft with crack. Use of the developed crack model in the algorithms of analysis of dynamic characteristics of aviation gas turbine engines rotors with cracks lowers significantly time that is necessary for its modeling and analysis. Analysis shows that crack in the shaft of the investigated rotor causes parametric resonances at the regimes  $1/3 \omega_{cr}$ ;  $1/2 \omega_{cr}$ ;  $1 \omega_{cr}$ , being the consequence of rotor harmonics with frequencies  $1x$ ,  $2x$ ,  $3x$ ,  $4x$ , etc. In the actual experiments it is possible to highlight two or three rotor harmonics. Presence of subharmonic resonances, multiple harmonics and change in motion orbits of the shafts sections can become signs of crack appearance.

Key words: rotor dynamics, crack, nonlinear model, Dynamics R4

## Introduction

The important direction in vibration diagnostics of aviation gas turbine engines and turbomachines is diagnostics through modelling. Modelling gives an opportunity to link the presence of some kinds of machine defects with signs of its presence in the vibration signal. One of such defects is crack appearance in the shafts of aviation engines and turbomachines which is unallowable. So the most important task of the diagnostic system is to detect crack in time and forecast its progress.

Appearance of crack in the rotor results in local stiffness decrease. Value of stiffness loss depends on geometric characteristics of crack. If static load such as weight force is applied, crack opens and closes while the rotor is rotating. As a result, the shaft stiffness changes per a cycle. Crack in the rotor system leads to the following changes in vibrational signal [1]:

- increase in amplitude of  $1x$  harmonic of rotating speed due to growth of static deflection caused by stiffness decrease.
- appearance of  $2x$  component of rotating speed due to asymmetric rotor stiffness.
- appearance of  $3x$  component of rotating speed due to cyclical opening and closing of crack.

The main task of the mathematical model is description of value and law of local change in stiffness in the place where crack takes place considering as many factors as possible.

There are several approaches to simulate crack. In the simplest cases crack is simulated by decrease in radial stiffness of the whole shaft [2,3,4]. In the other cases the shaft part, where crack takes place, is replaced by an equivalent beam element. Coefficients of stiffness matrix of such element are calculated taking crack into account and change per a cycle. In work [5] calculation of stiffness matrix of the beam element with crack is based on use of inertia moments of the beam section considering crack. In work [6] stiffness matrix of such element is calculated on the basis of equations of mechanics of solid bodies' destruction. Crack may be simulated by elastic link connecting boundary sections of the shaft in the place of its location and giving the crack moment stiffness [7,8].

Change in crack stiffness depending on its opening and closing while the rotor is rotating may be described mathematically in different ways. In the simplest case it may be assumed that crack has only two positions: entirely

opened or completely closed, and step function may be applied to describe its stiffness change mathematically [4].

Work [3] describes the most spread models of stiffness change. One of them is Gasch equation. Change in stiffness takes place depending on the angle between phase of static force and crack phase and described by 17 harmonics of Fourier series. The same article gives Maes & Davies equation where stiffness changes depending on angle according to cosine law. In the Yang model stiffness changes by the cosine law in degree of relative crack depth.

This article develops the crack model on the basis of existed approaches and also presents the methodology that gives opportunity to highlight signs used to detect its condition for the exact rotor.

The algorithm is included into the Dynamics R4 software program [9], which represents the dedicated system on calculation of dynamic behavior of complex rotor systems.

## Crack model

Within the accepted simulation conception, crack in the shaft model is replaced by an elastic link dividing the shaft into two sections and describing by stiffness matrix with variable coefficients. If there is no crack, strain compatibility condition between the sections of the shaft parts is accomplished, so all the mutual displacements are prohibited. We introduce the rotating coordinate system  $\eta\theta\varepsilon$  lying in the crack area, Figure 1. Its origin coincides with the origin of the fixed coordinate system  $XYZ$ . The shaft executes two motions – proper rotation and precession around  $Z$  axis. When describing crack we consider only rotation around  $\eta$  and  $\varepsilon$  axes. Displacements at other freedom degrees are neglected.

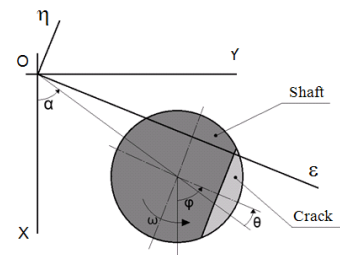


Figure 1. Crack section

Flexibility matrix of the link simulating crack in the rotating coordinate system may be written as the following:

$$[G_R(\theta)] = \begin{bmatrix} 0 & 0 & 0 & 0 & 0 & 0 \\ 0 & 0 & 0 & 0 & 0 & 0 \\ 0 & 0 & 0 & 0 & 0 & 0 \\ 0 & 0 & 0 & g_{\varepsilon\varepsilon}(\theta) & 0 & 0 \\ 0 & 0 & 0 & 0 & g_{\eta\eta}(\theta) & 0 \\ 0 & 0 & 0 & 0 & 0 & 0 \end{bmatrix}, \quad (1)$$

where  $\theta = \varphi - \alpha$  - difference in phases,  $\varphi$  - shaft rotation angle,  $\alpha$  - precession angle;  $g_{\varepsilon\varepsilon}(\theta)$  and  $g_{\eta\eta}(\theta)$  - variable coefficients of moment flexibility.

Flexibility depends on angle  $\theta$  because while the shaft is rotating, crack opens and closes. Stiffness matrix is obtained by inversion of the  $[G_R(\theta)]$  matrix, and zero flexibility coefficients at the main diagonal lead to obtainment of stiffness coefficients going to infinity. We limit value of such stiffness coefficients by  $1e10$  N/m; this assumption does not affect significantly the result, i.e. we obtain

$$[K_R(\theta)] = \begin{bmatrix} 1e10 & 0 & 0 & 0 & 0 & 0 \\ 0 & 1e10 & 0 & 0 & 0 & 0 \\ 0 & 0 & 1e10 & 0 & 0 & 0 \\ 0 & 0 & 0 & k_{\varepsilon\varepsilon}(\theta) & 0 & 0 \\ 0 & 0 & 0 & 0 & k_{\eta\eta}(\theta) & 0 \\ 0 & 0 & 0 & 0 & 0 & 1e10 \end{bmatrix}, \quad (2)$$

Stiffness matrix is transformed into the fixed coordinate system using the following equation:

$$[K(\theta, \varphi)] = [T]^T \cdot [K_R(\theta)] \cdot [T], \quad (3)$$

where  $[T]$  - rotation matrix (4), where  $C_1 = \cos(\varphi)$ ,  $S_1 = \sin(\varphi)$ .

$$[T] = \begin{bmatrix} C_1 & S_1 & 0 & 0 & 0 & 0 \\ -S_1 & C_1 & 0 & 0 & 0 & 0 \\ 0 & 0 & 1 & 0 & 0 & 0 \\ 0 & 0 & 0 & C_1 & S_1 & 0 \\ 0 & 0 & 0 & -S_1 & C_1 & 0 \\ 0 & 0 & 0 & 0 & 0 & 1 \end{bmatrix}, \quad (4)$$

Multiplying matrixes in correspondence with the equation (3) we obtain:

$$[K(\theta, \varphi)] = \begin{bmatrix} 1e10 & 0 & 0 & 0 & 0 & 0 \\ 0 & 1e10 & 0 & 0 & 0 & 0 \\ 0 & 0 & 1e10 & 0 & 0 & 0 \\ 0 & 0 & 0 & k_{\varepsilon\varepsilon}(\theta)C_1^2 + k_{\eta\eta}(\theta)S_1^2 & k_{\varepsilon\varepsilon}(\theta)C_1S_1 - k_{\eta\eta}(\theta)C_1S_1 & 0 \\ 0 & 0 & 0 & k_{\varepsilon\varepsilon}(\theta)C_1S_1 - k_{\eta\eta}(\theta)C_1S_1 & k_{\eta\eta}(\theta)C_1^2 + k_{\varepsilon\varepsilon}(\theta)S_1^2 & 0 \\ 0 & 0 & 0 & 0 & 0 & 1e10 \end{bmatrix}, \quad (5)$$

We carry out some transformations that give opportunity to pass to the simpler description of the crack stiffness matrix and the algorithm of its coefficients obtainment. In correspondence with the Maes model, it may be assumed that radial flexibility of the circular beam

with crack changes from minimum to maximum value by cosine law.

$$g(\theta) = \frac{(g_0 + g_c)}{2} + \frac{(g_0 - g_c)}{2} \cos(\theta), \quad (6)$$

where  $g_0$  - flexibility of the beam without crack (minimum value),  $g_c$  - flexibility of the beam with open crack (maximum value).

We replace crack by a hinge with moment stiffness  $k_{m_h}^{init}$ . The beam boundary conditions should provide its statal definability as it shown in Figure 2.

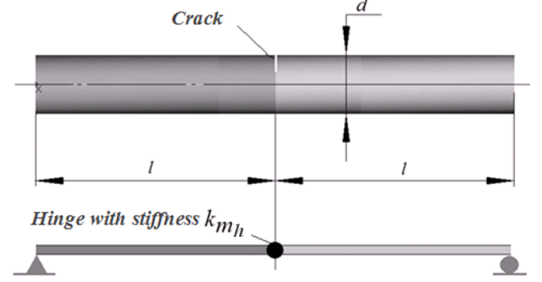


Figure 2. Replacement of crack by hinge

Then radial flexibility of highlighted section of the shaft with open crack is obtained as:

$$g_c = \frac{l^2}{4 \cdot k_{m_h}^{init}} + \frac{1}{6} \cdot \frac{l^3}{EI} \quad (7)$$

where  $E$  - Young modulus,  $I$  - diametral inertia moment of the shaft section,  $k_{m_h}^{init}$  - coefficient of moment stiffness of an equivalent link corresponding to fully open crack.

The equation has two summands - flexibility related to crack and flexibility of the beam without crack. It should be noted that irrespective of the beam shape, boundary conditions and the crack position, its contribution to general beam flexibility depends only on the coefficient  $k_{m_h}^{init}$ , i.e. the first summand.

While the beam is rotating, flexibility in the crack section changes. We obtain the following:

$$g(\theta) = \frac{l^2}{4 \cdot k_{m_h}(\theta)} + g_0, \quad (8)$$

where  $g_0 = \frac{1}{6} \cdot \frac{l^3}{EI}$  - flexibility of the beam without crack,  $k_{m_h}(\theta)$  - current coefficient of moment stiffness for the given  $\theta$ .

Integrating two equations (5) and (7), we obtain:

$$\frac{(g_0 + g_c)}{2} + \frac{(g_0 - g_c)}{2} \cos(\theta) = \frac{l^2}{4 \cdot k_{m_h}(\theta)} + g_0, \quad (9)$$

where taking the equation (6) into account we obtain the law of change in moment stiffness depending on difference in phases  $\theta$ :

$$k_{m_h}(\theta) = \frac{2 \cdot k_{m_h}^{init}}{(1 - \cos(\theta))}, \quad (10)$$

The obtained moment stiffness of an equivalent link depends only on the shaft diameter, material characteristics and the crack depth. Change in crack position in the shaft, characteristics of the shaft including the support units does not change moment stiffness of an equivalent link (on condition that the section with crack remains the same in any part of the section with crack for which it was obtained).

Going back to stiffness matrix obtained before, its stiffness coefficients may be written as the following:

$$k_{\varepsilon\varepsilon}(\theta) = \frac{2 \cdot k_{\varepsilon\varepsilon}^{init}}{(1 - \cos(\theta))}, \quad (11)$$

$$k_{\eta\eta}(\theta) = \frac{2 \cdot k_{\eta\eta}^{init}}{(1 - \cos(\theta))}, \quad (12)$$

where  $k_{\varepsilon\varepsilon}^{init}$ ,  $k_{\eta\eta}^{init}$  - initial values of moment stiffness at the corresponding axes for the fully open crack.

The task of  $k_{\varepsilon\varepsilon}^{init}$ ,  $k_{\eta\eta}^{init}$  calculation may be solved in two ways. The first one is calculation of moment stiffness in FEM program. The second one is to use the theory of fracture mechanics. It gives an opportunity to calculate values of coefficients of local flexibility of open crack if its geometry, the shaft diameter and material characteristics are known [7,10].

#### Algorithm to simulate rotor system with crack

The following steps should be passed to obtain coefficients of moment stiffness of the crack.

1. The complete rotor model is created in one of the specialized programs to analyze rotor dynamics (for example, in Dynamics R4).

2. The rotor section with crack is highlighted.

3. Crack divides the shaft section into two subsystems. Link described by the matrix of variable stiffness coefficients  $[K(\theta, \varphi)]$  by dimension 6x6 is placed between subsystems.

4. Initial coefficients of moment stiffness  $k_{\varepsilon\varepsilon}^{init}$ ,  $k_{\eta\eta}^{init}$  for open crack are obtained by the methods given above. These data are initial for calculation.

Stiffness matrix coefficients of the link simulating crack are calculated while integrating of motion equations of the rotor system for every  $\theta$ . At nonlinear statement matrix equation describing the nonlinear dynamic model of the rotor system is the following:

$$[M]\{\ddot{u}\} + [C]\{\dot{u}\} + [K]\{u\} = \{F(t)\}, \quad (13)$$

where  $[M]$  – matrix of inertia coefficients;  $[C]$  – matrix of damping and gyroscopes coefficients;  $[K]$  –

matrix of stiffness coefficients;  $\{\ddot{u}\}$ ,  $\{\dot{u}\}$ ,  $\{u\}$  – columns of vibrational accelerations, vibrational speeds and vibrational displacements correspondingly;  $\{F(t)\}$  – any types of dynamic loads– internal and external.

Stiffness matrix of an equivalent link may be divided into two parts: constant and variable, and the following is true:

$$[K(\theta, \varphi)] = [K_c] + [K_v(\theta, \varphi)] = \begin{bmatrix} 1e10 & 0 & 0 & 0 & 0 & 0 \\ 0 & 1e10 & 0 & 0 & 0 & 0 \\ 0 & 0 & 1e10 & 0 & 0 & 0 \\ 0 & 0 & 0 & 0 & 0 & 0 \\ 0 & 0 & 0 & 0 & 0 & 0 \\ 0 & 0 & 0 & 0 & 0 & 1e10 \end{bmatrix} + \begin{bmatrix} 0 & 0 & 0 & 0 & 0 & 0 \\ 0 & 0 & 0 & 0 & 0 & 0 \\ 0 & 0 & 0 & 0 & 0 & 0 \\ 0 & 0 & k_{\varepsilon\varepsilon}(\theta)C_1^2 + k_{\eta\eta}(\theta)S_1^2 & k_{\varepsilon\varepsilon}(\theta)C_1S_1 - k_{\eta\eta}(\theta)C_1S_1 & 0 \\ 0 & 0 & k_{\varepsilon\varepsilon}(\theta)C_1S_1 - k_{\eta\eta}(\theta)C_1S_1 & k_{\eta\eta}(\theta)C_1^2 + k_{\varepsilon\varepsilon}(\theta)S_1^2 & 0 \\ 0 & 0 & 0 & 0 & 0 & 0 \end{bmatrix} \quad (14)$$

$[K_c]$  is included into the general stiffness matrix of the  $[K]$  system. Matrix  $[K_v(\theta, \varphi)]$  is used to calculate reactions of a nonlinear link:

$$\{R\} = \begin{bmatrix} k_{\varepsilon\varepsilon}(\theta)C_1^2 + k_{\eta\eta}(\theta)S_1^2 & k_{\varepsilon\varepsilon}(\theta)C_1S_1 - k_{\eta\eta}(\theta)C_1S_1 \\ k_{\varepsilon\varepsilon}(\theta)C_1S_1 - k_{\eta\eta}(\theta)C_1S_1 & k_{\eta\eta}(\theta)C_1^2 + k_{\varepsilon\varepsilon}(\theta)S_1^2 \end{bmatrix} \begin{Bmatrix} u_{rx} \\ u_{ry} \end{Bmatrix}, \quad (15)$$

where  $u_{rx}$ ,  $u_{ry}$  – mutual rotations of the sections around the corresponding axes.

The final motion equation of the system is the following:

$$[M]\{\ddot{u}\} + [C]\{\dot{u}\} + [K]\{u\} = \{F(t)\} + \{R\}. \quad (16)$$

The given equation may be solved by numerical methods such as Runge-Kutta method, Newmark method, etc.

Adequacy of the suggested algorithm is done by comparison of flexibility of the two-support beam with crack obtained in the finite-element system and according to the supposed algorithm in Dynamics R4. The task is to calculate the beam deflection under unit force in the crack sections for different phases between crack and force.

Figure 3 shows the results of check of the suggested algorithm. Three results are compared:

- flexibility is calculated using the finite element method (FEM). Radial flexibility of the model of the beam with crack is calculated in the FEM-system for the whole range of angular positions of crack;

- flexibility is calculated using Dynamics R4, initial data are obtained using FEM. Initial values of moment stiffness for the fully open crack  $k_{\varepsilon\varepsilon}^{init}$ ,  $k_{\eta\eta}^{init}$  are obtained

solving equation (7) for  $k_{m_h}^{init}$ , and radial flexibility of the beam with crack  $g_c$  at the corresponding direction is calculated using FEM. Moment stiffness for the intermediate angular crack positions changes from minimum to maximum according to the (10) law;

- flexibility is calculated using Dynamics R4. Initial data of moment flexibility for fully open crack  $k_{\varepsilon\varepsilon}^{init}$ ,  $k_{\eta\eta}^{init}$  are obtained analytically using the algorithms of fracture mechanics [7, 10]. Value of moment flexibility for intermediate angular crack positions changes from minimum to maximum according to the law (10).

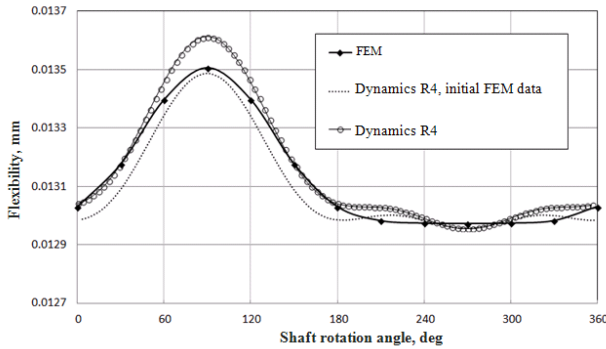


Figure 3 Change in beam flexibility in crack section per a revolution

The results in calculation of FEM-model and models in Dynamics R4 are close. Calculation results with initial conditions obtained analytically differ from the FEM results less than 1%. At the same time, initial stiffness is calculated analytically much faster than FEM calculation and requires less working hours and so easier-to-use.

#### Geometry and parameters of rotor with crack

Geometry of the rotor with crack is chosen to show the algorithm work to the best advantage, Table 1. The rotor with the central disc, the supports are placed at the shaft ends.

Table 1

Parameter	Numerical value
Shaft length, mm	400
Shaft diameter, mm	10
Density of shaft material, kg/m <sup>3</sup>	7800
Elasticity module of shaft material, N/m <sup>2</sup>	2,1·10 <sup>11</sup>
Radial stiffness of supports, N/m	1,3·10 <sup>8</sup>
Crack position, mm	200
Disk mass, kg	0,875
Polar inertia moment of disk, kg·m <sup>2</sup>	0,000634
Diametric inertia moment of disk, kg·m <sup>2</sup>	0,000365
Elasticity modulus of disk material, N/m <sup>2</sup>	2,1·10 <sup>11</sup>
Crack position, mm	200
Crack depth, mm	3

#### Simulation results

To show crack influence on dynamic rotor behavior, rotor acceleration was calculated in the range from 0 to 4000 rpm. Only weight force has outer influence. The first critical speed of such rotor accounts for  $\omega_{cr}=2643,6$  rpm (44,06 Hz). Figure 4 shows the obtained amplitude-frequency characteristics.

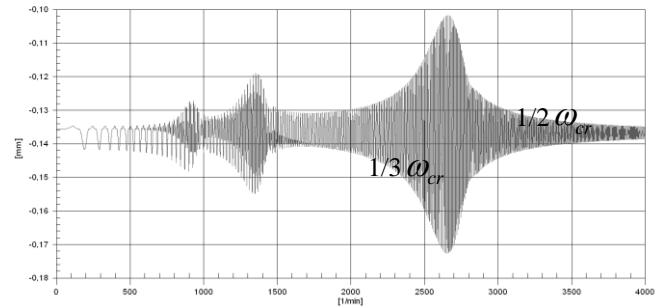


Figure 4. Amplitude-frequency characteristics in crack section

At 1/3 and 1/2 from critical speed, parametrical resonances being the result of cyclic change in moment stiffness appear. Cascade diagram shows 1x, 2x and 3x rotor harmonics, Figure 5.

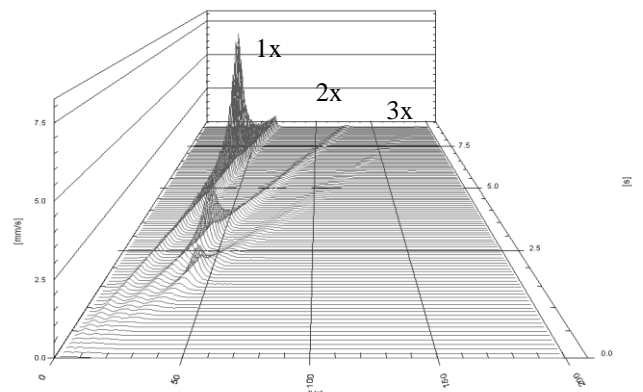


Figure 5. Cascade diagram of vibration speed while rotor accelerating up to 4000 rpm

Dynamic rotor characteristics (spectra and orbits) are given below at regimes  $\omega = 1/3\omega_{cr}$ ,  $\omega = 1/2\omega_{cr}$ ,  $\omega = \omega_{cr}$ . Only rotor weight represents outer loads.

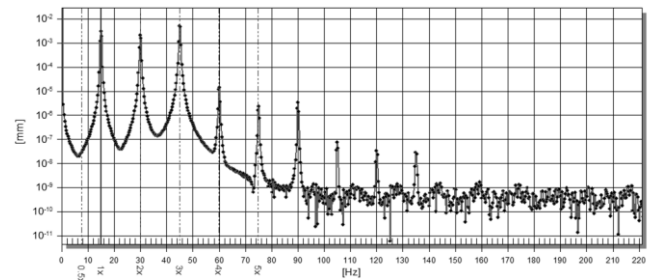


Figure 6 Signal spectrum at  $1/3 \omega_{cr}$  regime in logarithmical coordinates

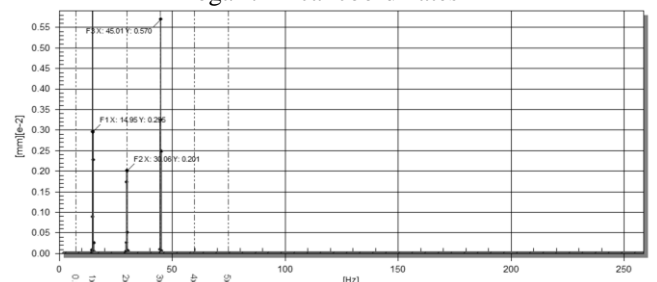


Figure 7 Signal spectra at  $1/3 \omega_{cr}$  regime in linear coordinates

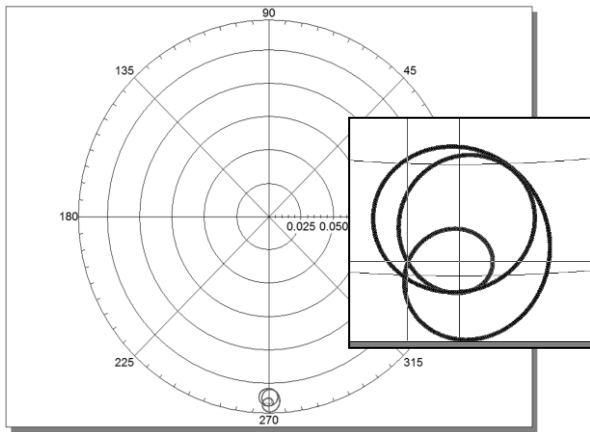


Figure 8 Orbits of rotor center in crack section at  $1/3 \omega_{cr}$  regime

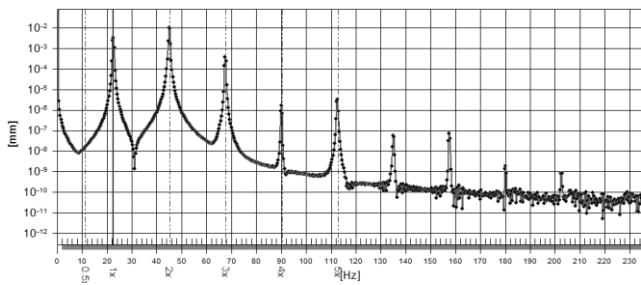


Figure 9 Signal spectra at  $1/2 \omega_{cr}$  regime in logarithmic coordinates

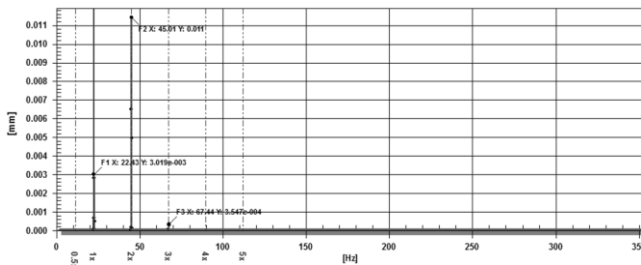


Figure 10 Signal spectrum at  $1/2 \omega_{cr}$  regime in linear coordinates

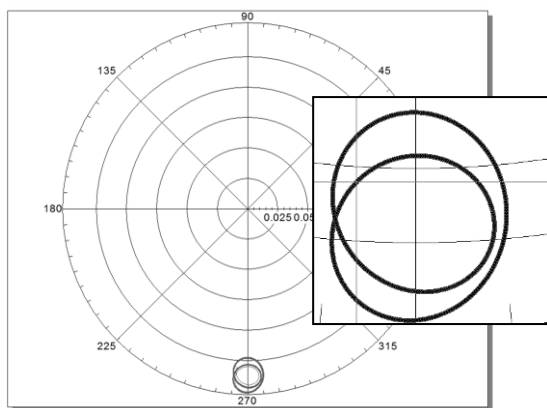


Figure 11 Orbits of rotor center in crack section at  $1/2 \omega_{cr}$  regime

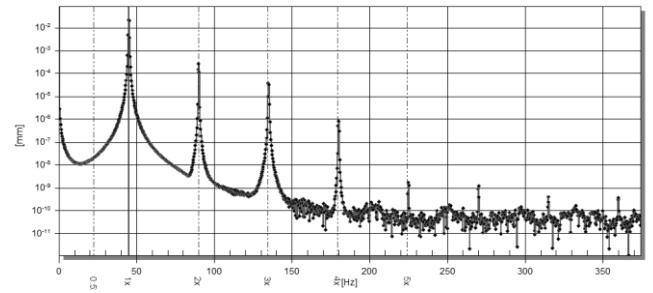


Figure 12 Signal spectra at  $\omega_{cr}$  regime in logarithmic coordinates

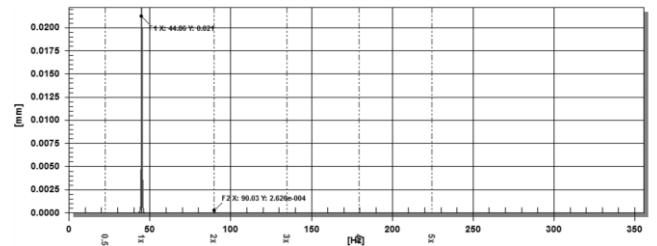


Figure 13 Signal spectra at  $\omega_{cr}$  regime in linear coordinates

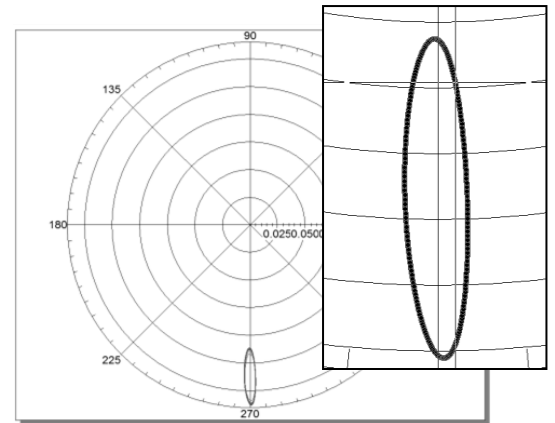


Figure 14 Orbits of rotor center in crack section at  $\omega_{cr}$  regime

Obtained results show that appearance of subharmonic resonances may be a diagnostic sign of crack appearance. The best diagnostic regime to detect multiple rotor harmonics is the regime of  $1/3$  from the first critical speed. Three harmonics of rotor frequency close in amplitudes value are seen at it.

### Conclusion

Use of the developed crack model in the algorithms of analysis of dynamic characteristics of rotors with crack lowers significantly time needed for their modeling and analysis. Calculation results show that crack in the shaft of the investigated rotor causes parametric resonances at regimes  $1/3 \omega_{cr}$ ,  $1/3 \omega_{cr}$ ,  $\omega_{cr}$  being the result of rotor harmonics with frequencies  $1x$ ,  $2x$ ,  $3x$ ,  $4x$ , etc. In actual tests there is an opportunity to highlight two or three rotor harmonics. Presence of subharmonic resonances, multiple harmonics and change in the motion orbit of the shaft sections may be signs of crack appearance. At the same

time it should be taken into account that probability to detect crack in actual practice depends on its geometry and depth, sensitivity of the used equipment, presence of orbits sensors, etc. So the proposed model should be considered mainly as an instrument to train engineers in the area of vibrational diagnostics, and to obtain limiting values of diagnostic signs of crack.

#### Literature

1. Bachschmid N., Pennacchi P., Tanzi E. Cracked rotors. Springer, 2010. 399 p.
2. J.E.T. Penny and M.I. Friswell. Simplified modelling of rotor cracks. Proceedings of ISMA 2002. Vol. 2. pp. 607-616.
3. J. Gomez-Mancilla, J.M. Machorro-Lopez and V.R. Nosov. Crack breathing mechanisms in rotor – bearing systems, its influence on system response and crack detection. ISCORMA – 3, Cleveland, Ohio, 19-23 September 2005. 10p.
4. O.S. Jun, H.J. Eun, Y.Y. Earmme, C.W. Lee. Modeling and vibration analysis of a simple rotor with a breathing crack. Journal of Sound and Vibration 155 (1992) pp. 273–290.
5. A.K. Darpe, K. Gupta, A. Chawla. Coupled bending, longitudinal and torsional vibrations of a cracked rotor. Journal of Sound and Vibration 269 (2004) pp. 33–60.
6. J.-J. Sinou and A.W. Lees. A non-linear study of a cracked rotor. European Journal of Mechanics - A/Solids. Vol. 26, Issue 1, January-February 2007, pp. 152-170.
7. A. C. Chasalevris. Vibration analysis of nonlinear-dynamic rotor-bearing systems and defect detection. Ph.D. Dissertation. University of Patras Press, 2009. 299p.
8. K.Kamiya, T.Yoshinaga. Nonlinear steady-state vibration analysis of a beam with breathing cracks (finite element analysis based on the mixed variation principle). Journal of System Design and Dynamics. Vol. 2, No.3, 2008 pp. 750-761.
9. Инженерно-консультационный центр по роторной динамике турбомашин различного назначения «Альфа - Транзит»: 2002-2014. URL: <http://www.rotordynamics.ru/>. (Дата обращения: 7.08.2014).
10. A. D. Dimarogonas and C. A. Papadopoulos. Vibration of cracked shafts in bending. Journal of Sound and Vibration 91(4) (1983), pp. 583-593.